Quadruple-Mode Coupled-Ring Resonator Bandpass Filter With Quasi-Elliptic Function Passband

U-Hou Lok, Yi-Chyun Chiou, *Student Member, IEEE*, and Jen-Tsai Kuo, *Senior Member, IEEE*

***Abstract*—Quadruple-mode coupled-ring resonator is used to design quasi-elliptic function bandpass filters (BPFs) with a relatively wide bandwidth. The resonator consists of a pair of coupled rings with two open stubs symmetrically tapped to the inner ring. The stubs are used to move a transmission zero near the center frequency to lower transition band. It is believed that it is the first ring resonator BPF based on the coupled-ring to create four transmission poles and four transmission zeros. Two filters with relative bandwidths of 10% and 15% are fabricated and measured. Good agreement between simulation and measurement is obtained.**

***Index Terms*—Bandpass filter (BPF), multimode resonator, planar circuit, quasi-elliptic function response, ring resonator.**

I. Introduction

MULTIMODE resonator bandpass filters (BPFs) have been a hot research topic recently [1]–[6]. Such resonator filters have many attractive features such as compact size, high selectivity and low cost. In the past, most of the reported multimode resonator filters have a three-dimensional configuration and usually occupy a large circuit volume [1], [2]. Recently, planar multimode resonators have been developed for ultra-wideband (UWB) [3]–[5] and broadband [6] filter designs. The ring resonator in [7] could be the first planar dual-mode element. Herein, there have been dual-mode BPFs with a miniaturized area [8], [9], a wide stopband [10], and tunable transmission zeros [11]. The bandwidth control of the circuit relies on a perturbation in the symmetric plane. Also, such filters have an attractive feature that two transmission zeros can be created on both sides of the passband by separating the input/output ports with a space of 90° [11].

In this letter, evolved from the traditional dual-mode ring resonator, a quadruple-mode coupled-ring resonator is developed to design a BPF with a quasi-elliptic passband and a relatively large bandwidth. In addition to the perturbation in the symmetric plane of the input/output feeds, two open stubs are attached to the inner ring to move a transmission zero from mid-passband to the lower transition band, so that an improved selectivity can be obtained.

Manuscript received August 30, 2007, revised November 13, 2007. This work was supported in part by the MoE ATU Program and by the National Science Council of Taiwan, R.O.C., under Grants NSC 95-2221-E-009-037-MY2 and NSC 96-2752-E-009-003-PAE.

The authors are with the Department of Communication Engineering, National Chiao Tung University, Hsinchu 300, Taiwan, R.O.C. (e-mail: jtkuo@mail.nctu.edu.tw).

Color versions of one or more of the figures in this letter are available online at http://ieeexplore.ieee.org.

Digital Object Identifier 10.1109/LMWC.2008.916782

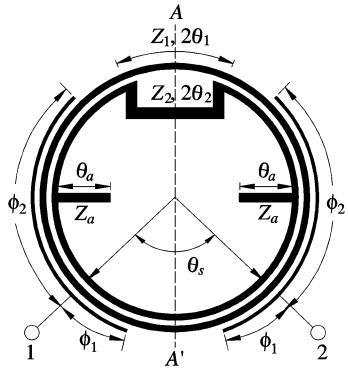

Fig. 1. Coupled-ring resonator with input/output line-to-ring couplers.

In the following, Section II investigates the resonant characteristics of the quadruple-mode resonator, Section III demonstrates the simulated and measured results of two fabricated BPFs, and Section IV draws the conclusion.

II. Resonant Characteristic of Coupled-Ring

Fig. 1 shows the layout of the proposed quadruple-mode coupled-ring resonator with input/output line-to-ring couplers. The uniform coupled-ring resonator will possess four degenerate modes. The circuit is symmetric about the A-A' plane which can be an electric and a magnetic wall for the odd and even mode analysis, respectively. The resonant frequencies ω_r can be approximated by [12]:

$$\frac{\omega_r}{v_c}\sqrt{\varepsilon_{eff}}\ell = \pi \tag{1}$$

where \ell is mean circumference of the coupled-ring, v_c is phase velocity of light in vacuum, and ε_{eff} is the effective dielectric constant of the even or odd mode on straight coupled microstrip lines. Since for coupled microstrips the even mode has a higher ε_{eff} value than the odd mode, the former will have a lower resonant frequency. In Fig. 1, the upper part of the ring (Z_2) is meandered or perturbed to separate the degenerate resonances. Two open stubs of electrical length θ_a are also attached to the inner ring. Their purpose will be addressed later.

With $\theta_a = 0$, Fig. 2 plots the leading four resonant frequencies, f_1 through f_4, normalized with respect to the fundamental frequency f_o of a single ring resonator with mean circumference l. The horizontal axis $u = \theta_1/\pi$ denotes amount of the perturbation. The two modes with $f_n/f_o > 1$ and the other two resonances with $f_n/f_o < 1$ correspond to the odd mode and even mode of the coupled lines, respectively. As shown in Fig. 2, the more the perturbation, the more the separation between the resonant frequencies of each pair.

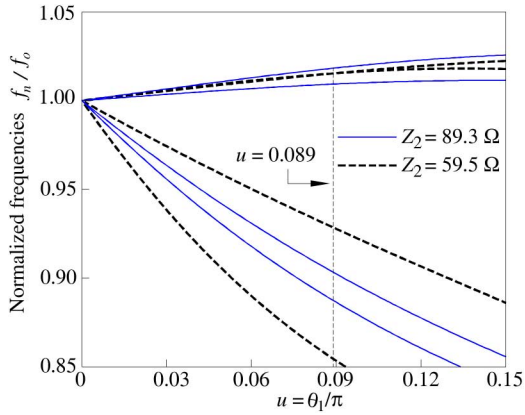

Fig. 2. Normalized resonant frequencies of the coupled-ring resonator. $Z_{oe} = 124\ \Omega$, $Z_{oo} = 55.7\ \Omega$, $Z_1 = 89.3\ \Omega$, $\theta_2/\theta_1 = 2$.

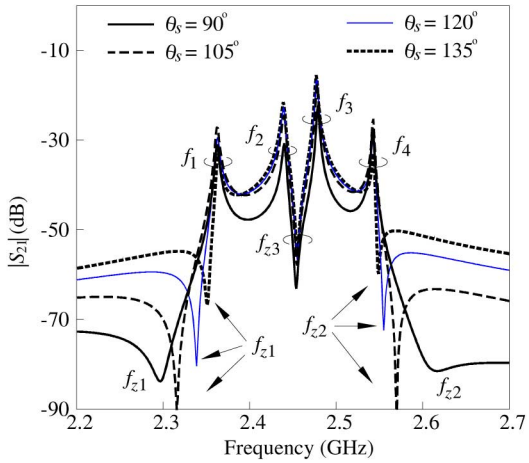

Fig. 3. Search for separation θ_s between the input/output couplers for the coupled-ring resonator BPF. $\theta_s = 90°$, 105°, 120° and 135°.

Fig. 3 tests the simulated $|S_{21}|$ responses for a coupled-ring resonator designed at center frequency $f_c = 2.45$ GHz with $\theta_s = 90°$, 105°, 120° and 135° and $\phi_1 = \phi_2 = 0°$. The substrate has $\varepsilon_r = 2.2$ and thickness $= 0.508$ mm. There are four resonant peaks, $f_1 \sim f_4$, and three zeros, $f_{z_1} \sim f_{z_3}$. The zero f_{z_3} and all the peaks are close to being independent of θ_s, while the zeros f_{z_1} and f_{z_2} move away from the passband as θ_s is decreased from 135° to 90°.

Note that the zero f_{z_3} locates near the center passband. It is due to that the outer ring is loaded by the inner one, so that the structure has a bandstop characteristic near f_c [13], [14]. The notch seriously blocks the passband synthesis and has to be moved to outside of the passband. The two shunt open stubs in Fig. 1 are employed to implement this purpose. Fig. 4(a) plots the variations of the poles and zeros versus $\theta_a/90°$ with $Z_a = 74.6\ \Omega$ and $Z_1 = 89.3\ \Omega$. Only f_3 and f_{z_3} move to lower frequencies as θ_a is increased, while all others are independent of θ_a. To utilize this property, θ_a is tuned so that the resonance f_3 is kept inside and f_{z_3} outside of the passband. As shown in Fig. 4(a), however, f_{z_3} is higher than f_3 until $\theta_a/90° = 0.26$ where both of them are less than f_{z_1}, i.e., outside of the passband. Thus, an extra perturbation (Z_1) is introduced to the outer

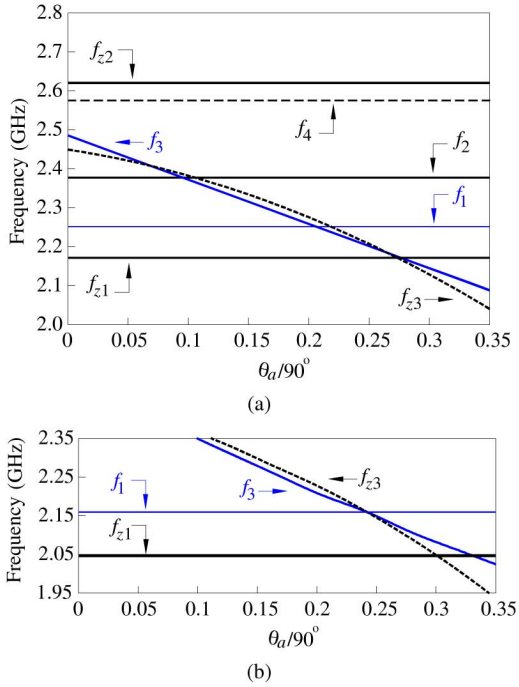

Fig. 4. Dependence of resonant and zero frequencies on the normalized stub length. $Z_{oe} = 124\ \Omega$, $Z_{oo} = 80.4\ \Omega$, $Z_2 = 88.2\ \Omega$, $Z_a = 74.6\ \Omega$, $\theta_2/\theta_1 = 2.33$. (a) $Z_1 = 89.3\ \Omega$. (b) $Z_1 = 55.7\ \Omega$.

ring to shift f_{z_1} down. Fig. 4(b) plots the variations of these frequencies versus θ_a with Z_1 being changed to 55.7 Ω. It can be seen that $f_{z_1} < f_{z_3} < f_3$ when $0.25 \le \theta_a/90° \le 0.30$.

III. Simulation and Measured Results

Two circuits are fabricated to validate the idea. The design procedure is similar to the multimode circuit in [6] and the BPF in [9]. Fig. 5(a) plots the simulated and measured results of the first quadruple-mode coupled-ring resonator BPF with $f_c = 2.45$ GHz and fractional bandwidth $\Delta = 10\%$ on a substrate of $\varepsilon_r = 2.2$ and thickness $= 0.508$ mm. Both line width and gap size of the line-to-ring coupling arm are 0.2 mm. The measured inband insertion loss and return loss are 1.1 dB and 17 dB, respectively. Note that there are four zeros near the passband, although one of them looks unclear. In comparison with those described above, the extra transmission zero could be generated by the length-to-ring coupled structures, i.e., ϕ_1 and ϕ_2 in Fig. 1. Simulation data for a traditional dual-mode ring resonator filter with the same 3-dB bandwidth are also shown for comparison. The proposed design indeed possesses much better selectivity in the transition bands.

Fig. 5(b) plots the simulated and measured results of the second BPF with $\Delta = 15\%$ on a substrate with $\varepsilon_r = 10.2$ and thickness $= 1.27$ mm. The width and gap size of the line-to-ring coupler are 0.15 mm and 0.14 mm, respectively. The zeros are measured at 2.11 GHz, 2.22 GHz, 2.7 GHz and 2.83 GHz. The measured inband $|S_{21}|$ and $|S_{11}|$ are -0.66 dB and -16.9 dB, respectively. Inside the passband, the four transmission poles can be clearly observed. Good agreement between simulation and measured results is obtained. Fig. 5(c) shows the photograph of the circuit in Fig. 5(b).

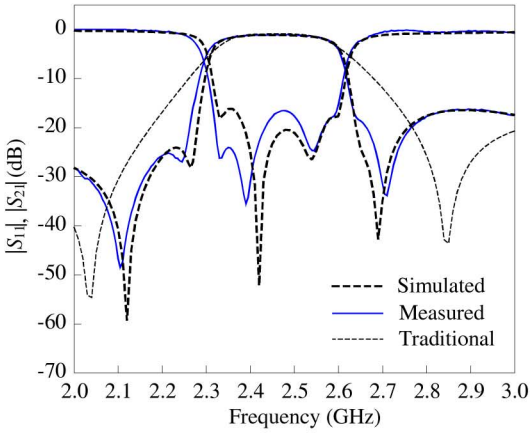

(a)

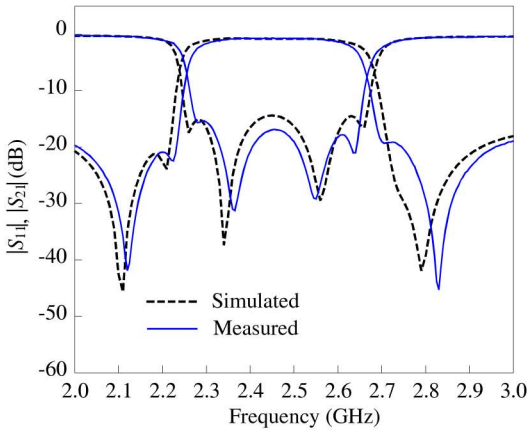

(b)

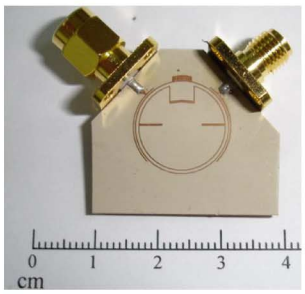

(c)

Fig. 5. Performance of two quadruple-mode coupled-ring resonator BPFs. (a) Filter 1: $\Delta = 10\%$. $Z_{oe} = 154\ \Omega$, $Z_{oo} = 80.4\ \Omega$, $Z_1 = 86.5\ \Omega$, $Z_2 = 79.5\ \Omega$, $Z_a = 73.0\Omega$, $u = 0.035$, $\theta_2/\theta_1 = 2.07$, $\theta_s = 90°$, $\theta_a = 16.6°$, $\phi_1 = 38°$ and $\phi_2 = 88°$. (b) Filter 2: $\Delta = 15\%$. $Z_{oe} = 124\ \Omega$, $Z_{oo} = 80.4\ \Omega$, $Z_1 = 55.7\ \Omega$, $Z_2 = 88.2\ \Omega$, $Z_a = 74.6\ \Omega$, $u = 0.089$, $\theta_2/\theta_1 = 2$, $\theta_s = 270°$, $\theta_a = 26.2°$, $\phi_1 = 101°$ and $\phi_2 = 12.5°$. (c) Photo of the circuit in (b).

IV. Conclusion

Design of ring resonator BPF with quadruple-mode coupled-ring resonator is proposed. Attached to the inner ring, two open stubs are used to shift a zero near the center frequency to transition band, which in turn improves the frequency selectivity of the circuit. In comparison with the traditional dual-mode ring resonator filter, the proposed circuit offers two more transmission poles in the passband and two more zeros in the stopband. It is thus a good candidate for design of quasi-elliptic function ring resonator filters with a relatively large bandwidth and improved selectivity.

References

[1] U. Rosenberg, "Multiplexing and double band filtering with common-multimode cavities," *IEEE Trans. Microw. Theory Tech.*, vol. 38, no. 12, pp. 1862–1871, Dec. 1990.

[2] W. Steyn and P. Meyer, "A shorted waveguide-stub coupling mechanism for narrow-band multimode coupled resonator filters," *IEEE Trans. Microw. Theory Tech.*, vol. 52, no. 6, pp. 1622–1625, Jun. 2004.

[3] S. W. Wong and L. Zhu, "EBG-embedded multiple-mode resonator for UWB bandpass filter with improved upper stopband performance," *IEEE Microw. Wireless Compon. Lett.*, vol. 17, no. 6, pp. 421–423, Jun. 2007.

[4] J. Gao, L. Zhu, W. Menzel, and F. Bogelsack, "Short-circuited CPW multiple-mode resonator for ultra-wideband (UWB) bandpass filter," *IEEE Microw. Wireless Compon. Lett.*, vol. 16, no. 3, pp. 104–106, Mar. 2006.

[5] L. Zhu, S. Sun, and W. Menzel, "Ultra-wideband (UWB) bandpass filter using multiple-mode resonator," *IEEE Microw. Wireless Compon. Lett.*, vol. 15, no. 11, pp. 796–798, Nov. 2006.

[6] Y.-C. Chiou, J.-T. Kuo, and E. Cheng, "Broadband quasi-Chebyshev bandpass filters with multimode stepped-impedance resonators (SIRs)," *IEEE Trans. Microw. Theory Tech.*, vol. 54, no. 8, pp. 3352–3358, Aug. 2006.

[7] I. Wolff, "Microstrip bandpass filter using degenerate modes of a microstrip ring resonator," *Electron. Lett.*, vol. 8, no. 12, pp. 302–303, Jun. 1972.

[8] J. S. Hong and M. J. Lancaster, "Microstrip bandpass filter using degenerate modes of a novel meander loop resonator," *IEEE Microw. Guided Wave Lett.*, vol. 5, no. 11, pp. 371–372, Nov. 1995.

[9] J.-T. Kuo and C.-Y. Tsai, "Periodic stepped-impedance ring resonator (PSIRR) bandpass filter with a miniaturized area and desirable upper stopband characteristics," *IEEE Trans. Microw. Theory Tech.*, vol. 54, no. 3, pp. 1107–1112, Mar. 2006.

[10] A. Görür, "A novel dual-mode bandpass filter with wide stopband using the properties of microstrip open-loop resonator," *IEEE Microw. Wireless Compon. Lett.*, vol. 12, no. 10, pp. 386–388, Oct. 2002.

[11] A. C. Kundu and I. Awai, "Control of attenuation pole frequency of a dual-mode microstrip ring resonator bandpass filter," *IEEE Trans. Microw. Theory Tech.*, vol. 49, no. 6, pp. 1113–1117, Jun. 2001.

[12] I. Wolff and W. Menzel, "The microstrip double-ring resonator," *IEEE Trans. Microw. Theory Tech.*, vol. MTT-23, no. 5, pp. 441–444, May 1975.

[13] L.-H. Hsieh and K. Chang, "Slow-wave bandpass filter using ring and stepped-impedance hairpin resonators," *IEEE Trans. Microw. Theory Tech.*, vol. 50, no. 7, pp. 1795–1800, Jul. 2002.

[14] J. Garcia-Garcia, F. Martin, F. Falcone, J. Bonache, I. Gil, T. Lopetegi, M. A. G. Laso, M. Sorolla, and R. Marques, "Spurious passband suppression in microstrip coupled line bandpass filter by means of split ring resonators," *IEEE Microw. Wireless Compon. Lett.*, vol. 14, no. 9, pp. 416–418, Sep. 2004.